Letter

How does the $X(3872)$ show up in e^+e^- collisions: Dip versus peak

Vadim Baru,[1,*] Feng-Kun Guo,[2,3,4,5,†] Christoph Hanhart,[6,‡] and Alexey Nefediev[7,8,§]

[1]*Institut für Theoretische Physik II, Ruhr-Universität Bochum, D-44780 Bochum, Germany*
[2]*CAS Key Laboratory of Theoretical Physics, Institute of Theoretical Physics, Chinese Academy of Sciences, Beijing 100190, China*
[3]*School of Physical Sciences, University of Chinese Academy of Sciences, Beijing 100049, China*
[4]*Peng Huanwu Collaborative Center for Research and Education, Beihang University, Beijing 100191, China*
[5]*Southern Center for Nuclear-Science Theory (SCNT), Institute of Modern Physics, Chinese Academy of Sciences, Huizhou 516000, China*
[6]*Institute for Advanced Simulation, Forschungszentrum Jülich, D-52425 Jülich, Germany*
[7]*Jozef Stefan Institute, Jamova 39, 1000 Ljubljana, Slovenia*
[8]*CeFEMA, Center of Physics and Engineering of Advanced Materials, Instituto Superior Técnico, Avenida Rovisco Pais 1, 1049-001 Lisboa, Portugal*

(Received 22 April 2024; accepted 16 May 2024; published 12 June 2024)

We demonstrate that the dip observed near the total energy of 3872 MeV in the recent cross section data from the BESIII Collaboration for $e^+e^- \to J/\psi\pi^+\pi^-$ admits a natural explanation as a coupled-channel effect: it is a consequence of unitarity and a strong S-wave $D\bar{D}^*$ attraction that generates the state $X(3872)$. We anticipate the appearance of a similar dip in the $e^+e^- \to J/\psi\pi^+\pi^-\pi^0$ final state near the $D^*\bar{D}^*$ threshold driven by the same general mechanism, then to be interpreted as a signature of the predicted spin-2 partner of the $X(3872)$.

DOI: 10.1103/PhysRevD.109.L111501

Since the first exotic state $\chi_{c1}(3872)$ [also known as $X(3872)$] in the spectrum of charmonium was discovered by the Belle Collaboration in 2003 [1], quarkoniumlike states have been under intensive studies as they provide a unique laboratory to test our understanding of excited hadrons and thus the nonperturbative regime of quantum chromodynamics (for reviews, we refer to Refs. [2–9]). Recent studies of the electron-positron annihilation in the energy range 3.8–3.9 GeV performed by the BESIII Collaboration revealed the appearance of a dip rather than peak in the line shape in the vicinity of the mass of $X(3872)$ [10].[1] We demonstrate in this Letter that this structure finds a natural explanation in the interplay of different production mechanisms operative for the $X(3872)$ production in e^+e^- collisions as a concrete realization of the universal mechanism introduced in Ref. [13].

The scene is set by two competing production channels, for definiteness referred to as channel 1 and channel 2, with the thresholds $E_1^{\rm thr}$ and $E_2^{\rm thr}$, respectively. In what follows, $E_2^{\rm thr} - E_1^{\rm thr} > 0$, and the energy E is counted from the higher threshold, $E_2^{\rm thr}$. We introduce:

(i) a_{11} as a parameter that governs the single-channel interaction strength in channel 1 at the threshold of channel 2,
(ii) a_{22} as the S-wave scattering length in channel 2 in case it is completely decoupled from channel 1,
(iii) a_{12} as the parameter that describes coupling of channels 1 and 2.

Then, the expression for the elastic scattering amplitude in channel 1 within the energy region around $E_2^{\rm thr}$ obtained in a nonrelativistic effective field theory for channel 2 reads [13]

$$T_{11}(E) = -8\pi E_2^{\rm thr}\left(\frac{1}{a_{11}^{-1} - ik_1} + \frac{a_{12}^{-2}(a_{11}^{-1} - ik_1)^{-2}}{a_{22,\rm eff}^{-1} - ik_2}\right), \tag{1}$$

where k_1 is the center-of-mass momentum in channel 1; $k_2 \approx \sqrt{2\mu_2 E}$ is the momentum in channel 2 treated nonrealativisitcally in the energy range of interest; μ_2 is the

*vadim.baru@tp2.rub.de
†fkguo@itp.ac.cn
‡c.hanhart@fz-juelich.de
§Alexey.Nefediev@ijs.si

[1]The same data point is also seen as a dip at the energy 3871.3 MeV in the data in Ref. [11]. No signal around the $X(3872)$ mass was seen in the $J/\psi\pi^+\pi^-$ invariant mass distribution of the initial-state radiation process $e^+e^- \to \gamma_{\rm ISR}J/\psi\pi^+\pi^-$ due to the low statistics [12].

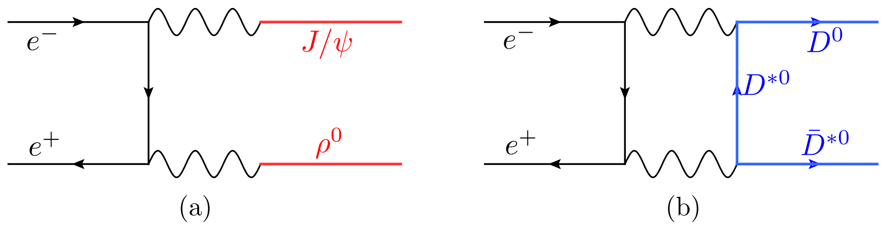

FIG. 1. The lowest-order diagrams for the $e^+e^- \to J/\psi\rho^0$ [diagram (a)] and $e^+e^- \to D^0\bar{D}^{*0}$ [diagram (b)] annihilation via two photons.

reduced mass in channel 2; and the effective scattering length in channel 2 coupled to channel 1, $a_{22,\mathrm{eff}}$, is given by

$$a_{22,\mathrm{eff}}^{-1} = a_{22}^{-1} - a_{12}^{-2}(a_{11}^{-1} - ik_1)^{-1}. \tag{2}$$

Notice that here channel 1 is not required to be nonrelativistic though the amplitude $T_{11}(E)$ takes the same form as that obtained when both channels are nonrelativistic [14].

The first term on the right-hand side in Eq. (1) can be regarded as a background coming from channel 1 alone. The channel coupling induces an interference, with the relative phase completely fixed by unitarity, that ensures the emergence of a dip in the line shape $|T_{11}|^2$ as long as $|a_{22}|$ is large enough. To see it explicitly, we employ relation (2) to bring the amplitude in Eq. (1) to the form

$$T_{11}(E) = \frac{-8\pi E_2^{\mathrm{thr}}(a_{22}^{-1} - i\sqrt{2\mu_2 E})}{(a_{11}^{-1} - ik_1)(a_{22,\mathrm{eff}}^{-1} - i\sqrt{2\mu_2 E})}, \tag{3}$$

where the numerator on the right-hand side vanishes at $E = 0$ for $a_{22} \to \infty$, the so-called unitary limit, while the denominator remains finite in this limit. The zero of T_{11} in Eq. (3) is an example of a Castillejo-Dalitz-Dyson zero [15]; see also Ref. [16]. In a more realistic situation, when the interaction in the decoupled channel 2 approaches the unitary limit (large $|a_{22}|$), the scattering amplitude in channel 1 must show a dip at the threshold of channel 2.

This universal picture allows one to interpret the well-known fact that the $f_0(980)$ appears as a dip in the $\pi\pi \to \pi\pi$ scattering amplitude (see, for example, Ref. [17]), where $\pi\pi$ and $K\bar{K}$ act as channels 1 and 2, respectively, as a necessary consequence of the strong S-wave $K\bar{K}$ attraction.

Similarly, a dip at an energy around 1.67 GeV in the $K^-p \to K^-p$ and $K^-p \to \bar{K}^0 n$ total cross sections (see the data compiled in Ref. [18]) may indicate a strong S-wave attraction in the $\Lambda\eta$ channel, whose threshold is at 1664 MeV. Further examples of near-threshold dip structures due to the same mechanism include a dip around the $\bar{K}N$ threshold in the $\pi\Sigma \to \pi\Sigma$ scattering amplitude from unitarized chiral perturbation theory (UChPT) [19,20] or lattice quantum chromodynamics [21], a dip around the $D_s^*\bar{K}$ threshold in the $D^*\pi \to D^*\pi$ scattering amplitude from UChPT [22], and so on. Below, we show that the same mechanism is at work in the direct production of the $X(3872)$ in e^+e^- collisions [see also Ref. [23] for an estimate of the $X(3872)$ dielectron width].

Recently, the cross section of the reaction $e^+e^- \to J/\psi\pi^+\pi^-$ was measured by the BESIII Collaboration at several energies [10], and contrary to naive expectations, no enhancement around the $X(3872)$ mass was observed. Instead, there is an indication of a dip, although the data are admittedly also consistent with a flat distribution [10]. Below, we provide theoretical arguments supporting the necessity for the appearance of this dip and emphasize the importance of further detailed studies to understand its manifestation in the data.

We denote $J/\psi\rho$ and $D\bar{D}^*$ as channel 1 and channel 2, respectively, and neglect the $J/\psi\omega$ channel for simplicity. We note that the $J/\psi\rho^0$ state with $J^{PC} = 1^{++}$ can be produced in e^+e^- collisions at tree level through two virtual photons [see Fig. 1(a)] while the state $D\bar{D}^*$ + c.c. with the same quantum numbers can only be produced at the loop level [see Fig. 1(b)]; thus, the latter is expected to be suppressed by the geometric factor $1/(16\pi^2)$.[2] Therefore, we neglect the direct production through the $D\bar{D}^*$ + c.c. channel and write the $e^+e^- \to J/\psi\rho^0$ amplitude in the vicinity of the $D\bar{D}^*$ threshold as

$$\mathcal{A}(\sqrt{s}) = P_0 + P_1 T_{11}(E), \tag{4}$$

where $\sqrt{s} = m_{D^0} + m_{D^{*0}} + E$ is the e^+e^- center-of-mass energy and the last term on the right-hand side describes rescatterings. In particular, it contains the $J/\psi\rho - D\bar{D}^*$ coupled-channel dynamics discussed above. Then, the $J/\psi\rho \to J/\psi\rho$ scattering amplitude T_{11} can be approximated by Eq. (3), and the corresponding cross section reads

$$\sigma(\sqrt{s}) = \mathcal{N}_0 \int_{-\infty}^{+\infty} dw \frac{|\mathcal{A}(\sqrt{s} - w)|^2}{\sqrt{2\pi}\delta_E} \exp\left(-\frac{w^2}{2\delta_E^2}\right), \tag{5}$$

where $\mathcal{N}_0$ is an overall normalization factor and the signal is convolved with a Gaussian-distributed energy spread to mimic the actual situation of the BESIII experiment, with

[2] We also recall that the magnetic vertex $\gamma D^0\bar{D}^{*0}$ is proportional to the D^0 momentum that vanishes at the $D^0\bar{D}^{*0}$ (channel-2) threshold.

TABLE I. Parameters of the best fits to the BESIII data [10]. The uncertainties are propagated from the experimental data only. Note that, while a_{22} was fitted to data, a_{11} and $|a_{12}|$ were then computed from a_{22} and the value of $a_{22,\mathrm{eff}}$ in Eq. (6).

	$\mathcal{N}$ (pb)	$R\times 10^2$	a_{22} (fm)	χ^2/dof	a_{11} (fm)	$\lvert a_{12}\rvert$ (fm)
Fit 1	$2.6^{+1.4}_{-1.1}$	$0.27^{+0.34}_{-0.29}$	$-6.6^{+2.8}_{-2.0}$	0.02	$-0.51^{+0.25}_{-0.22}$	$1.8^{+0.5}_{-0.8}$
Fit 2	$0.18^{+0.09}_{-0.07}$	$5.9^{+3.2}_{-2.3}$	$-10.8^{+2.0}_{-6.6}$	0.18	$-1.0^{+0.3}_{-1.7}$	$2.8^{+0.7}_{-0.4}$
Fit 3	$0.41^{+0.23}_{-0.16}$	$-2.6^{+1.0}_{-1.5}$	$-12.8^{+3.2}_{-13.2}$	0.15	$-1.4^{+0.5}_{-19.8}$	$3.1^{+0.6}_{-0.5}$

the energy spread $\delta_E = 1.7$ MeV [10]. Since the energy range of interest is narrow (from 3.8 to 3.9 GeV), only the leading energy dependence is retained in Eq. (5), while the overall kinematical factor is treated as a constant for simplicity.

Since P_0 can be absorbed by the overall normalization, $\mathcal{N}\equiv P_0^2\mathcal{N}_0$, the resulting model depends on five real parameters: $\{a_{11}, a_{12}, a_{22}, R, \mathcal{N}\}$, where $R\equiv P_1/P_0$. Using the results of Ref. [24] and the data in Ref. [25], the $D\bar{D}^*$ scattering length in the $X(3872)$ channel is determined to be

$$a_{22,\mathrm{eff}} = (-6.39 + i11.74)\ \mathrm{fm}. \tag{6}$$

Then, in the considered two-channel formalism, Eq. (2) constrains two real parameters (we choose them to be a_{11} and a_{12}) through the third one (a_{22}). In particular, we use

$$a_{11}^{-1} = k_1\frac{\mathrm{Re}(a_{22,\mathrm{eff}}^{-1}) - a_{22}^{-1}}{\mathrm{Im}(a_{22,\mathrm{eff}}^{-1})} \tag{7}$$

in the amplitude T_{11} in Eq. (3), while the channel-coupling parameter can be obtained as

$$a_{12}^{-1} = \sqrt{\frac{k_1}{\mathrm{Im}(a_{22,\mathrm{eff}})}}\left|1 - \frac{a_{22,\mathrm{eff}}}{a_{22}}\right|. \tag{8}$$

To take into account a finite width of the ρ meson, we evaluate the momentum k_1 as [26,27]

$$k_1 = \mathrm{Re}\sqrt{\frac{[s-(m_{J/\psi}+m_\rho)^2][s-(m_{J/\psi}-m_\rho)^2]}{4s}}, \tag{9}$$

with $m_\rho = (775 - i75)$ MeV, and it is evaluated at the $D^0\bar{D}^{*0}$ threshold in Eqs. (7) and (8). Notice that to fit to the BESIII data over the energy range from about 3.81 to 3.9 GeV we keep the full expression for k_1 in Eq. (9) and do not expand it in powers of E.

Then, the BESIII data from Ref. [10] are fitted using Eq. (5) with T_{11} from Eq. (3) and with the three free parameters in the fit being $\{\mathcal{N}, R, a_{22}\}$—their fitted values are listed in Table I. The line shapes for the three best fits are depicted in Fig. 2. A well-pronounced dip at the $D\bar{D}^*$ threshold is clearly seen in all three line shapes.

We conclude that the measured $X(3872)$ line shape is well described by the $J/\psi\rho^0 - D\bar{D}^*$ coupled-channel rescattering mechanism outlined above. Although the parameters of the three fits differ substantially from each other, all fits provide equally decent description of the data and possess common gross features. In particular, the three line shapes are nearly indistinguishable in the proximity of the $D\bar{D}^*$ threshold where they all show a pronounced dip. The large absolute and negative values of a_{22} found in all three fits imply a loosely bound $D\bar{D}^*$ state in the single-channel case. Additional data in the vicinity of the $D\bar{D}^*$ threshold would allow us to better constrain the model and extract the interaction strengths in different channels with higher precision. Also, we emphasize that, while particular details of the line shape in the $e^+e^- \to J/\psi\pi^+\pi^-$ production reaction depend on a delicate interplay of several parameters, the main mechanism driving the dip at the $D\bar{D}^*$ threshold is general and is controlled by the large scattering length in this channel.

At leading order in heavy quark spin symmetry, the $D\bar{D}^*$ interaction with $J^{PC} = 1^{++}$ agrees with that of $D^*\bar{D}^*$ with $J^{PC} = 2^{++}$. Accordingly, if the former interaction generates the $X(3872)$, the latter is predicted to generate its spin-2 partner state [28–30]. We therefore predict an

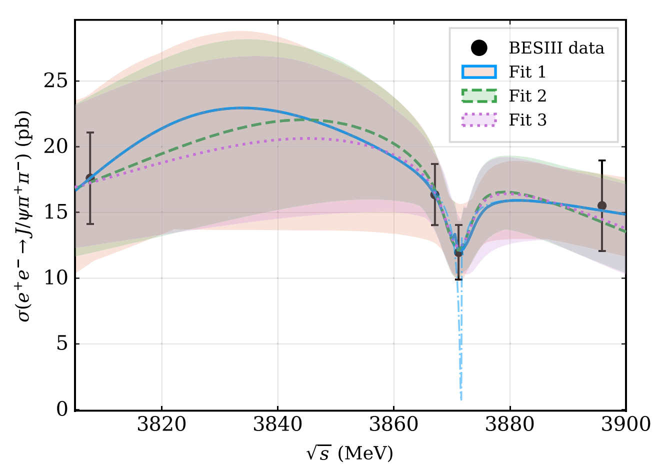

FIG. 2. The line shapes for the three best fits in Table I to the BESIII data [10] for the $e^+e^- \to J/\psi\pi^+\pi^-$ annihilation after convolution with the energy spread function—see Eq. (5). As an example, the blue dashed line shows the line shape for fit 1 without the effect of the energy spread. The 1σ error bands correspond to the uncertainty propagated from the data.

analogous dip as discussed above near the $D^*\bar{D}^*$ threshold in the production process $e^+e^- \to J/\psi\pi^+\pi^-\pi^0$. We notice that the cross section of $e^+e^- \to X_2(4014)$ has been estimated to be $\mathcal{O}(10 \text{ pb})$ under the assumption that the $X_2(4014)$ is a $D^*\bar{D}^*$ molecule [31]. Given that, the predicted dip may be observed at the upcoming BEPC II-U [32], which will have a luminosity three times that of BEPC II, and at the Super τ-Charm Facility [33].

We would like to thank Henryk Czyż, Achim Denig, Meng-Lin Du, and Chang-Zheng Yuan for useful discussions. This work is supported in part by the National Key R&D Program of China under Grant No. 2023YFA1606703; by the Chinese Academy of Sciences (CAS) under Grant No. YSBR-101; by the National Natural Science Foundation of China under Grants No. 12125507, No. 12361141819, and No. 12047503; and by NSFC and the Deutsche Forschungsgemeinschaft through the funds provided to the Sino-German Collaborative Research Center CRC110 "Symmetries and the Emergence of Structure in QCD" (DFG Project No. 196253076). Work of A. N. was supported by the Slovenian Research Agency (research core Funding No. P1-0035) and the CAS President's International Fellowship Initiative (Grant No. 2024PVA0004).

[1] S. K. Choi *et al.* (Belle Collaboration), Observation of a narrow charmonium-like state in exclusive $B^\pm \to K^\pm\pi^+\pi^- J/\psi$ decays, Phys. Rev. Lett. **91**, 262001 (2003).
[2] A. Hosaka, T. Iijima, K. Miyabayashi, Y. Sakai, and S. Yasui, Exotic hadrons with heavy flavors: X, Y, Z, and related states, Prog. Theor. Exp. Phys. **2016**, 062C01 (2016).
[3] R. F. Lebed, R. E. Mitchell, and E. S. Swanson, Heavy-quark QCD exotica, Prog. Part. Nucl. Phys. **93**, 143 (2017).
[4] A. Esposito, A. Pilloni, and A. D. Polosa, Multiquark resonances, Phys. Rep. **668**, 1 (2017).
[5] F.-K. Guo, C. Hanhart, U.-G. Meißner, Q. Wang, Q. Zhao, and B.-S. Zou, Hadronic molecules, Rev. Mod. Phys. **90**, 015004 (2018).
[6] S. L. Olsen, T. Skwarnicki, and D. Zieminska, Nonstandard heavy mesons and baryons: Experimental evidence, Rev. Mod. Phys. **90**, 015003 (2018).
[7] Y. S. Kalashnikova and A. V. Nefediev, X(3872) in the molecular model, Phys. Usp. **62**, 568 (2019).
[8] N. Brambilla, S. Eidelman, C. Hanhart, A. Nefediev, C.-P. Shen, C. E. Thomas, A. Vairo, and C.-Z. Yuan, The XYZ states: Experimental and theoretical status and perspectives, Phys. Rep. **873**, 1 (2020).
[9] H.-X. Chen, W. Chen, X. Liu, Y.-R. Liu, and S.-L. Zhu, An updated review of the new hadron states, Rep. Prog. Phys. **86**, 026201 (2022).
[10] M. Ablikim *et al.* (BESIII Collaboration), Measurement of the $e^+e^- \to \pi^+\pi^- J/\psi$ cross section in the vicinity of 3.872 GeV, Phys. Rev. D **107**, 032007 (2023).
[11] M. Ablikim *et al.* (BESIII Collaboration), Study of the resonance structures in the process $e^+e^+ \to \pi^+\pi^- J/\psi$, Phys. Rev. D **106**, 072001 (2022).
[12] M. Ablikim *et al.* (BESIII Collaboration), An improved limit for Γ_{ee} of $X(3872)$ and Γ_{ee} measurement of $\psi(3686)$, Phys. Lett. B **749**, 414 (2015).
[13] X.-K. Dong, F.-K. Guo, and B.-S. Zou, Explaining the many threshold structures in the heavy-quark hadron spectrum, Phys. Rev. Lett. **126**, 152001 (2021).
[14] T. D. Cohen, B. A. Gelman, and U. van Kolck, An effective field theory for coupled channel scattering, Phys. Lett. B **588**, 57 (2004).
[15] L. Castillejo, R. H. Dalitz, and F. J. Dyson, Low's scattering equation for the charged and neutral scalar theories, Phys. Rev. **101**, 453 (1956).
[16] C. Hanhart, Y. S. Kalashnikova, and A. V. Nefediev, Interplay of quark and meson degrees of freedom in a near-threshold resonance: Multi-channel case, Eur. Phys. J. A **47**, 101 (2011).
[17] L.-Y. Dai and M. R. Pennington, Comprehensive amplitude analysis of $\gamma\gamma \to \pi^+\pi^-, \pi^0\pi^0$ and $\bar{K}K$ below 1.5 GeV, Phys. Rev. D **90**, 036004 (2014).
[18] H. Kamano, S. X. Nakamura, T. S. H. Lee, and T. Sato, Dynamical coupled-channels model of K^-p reactions. II. Extraction of Λ^* and Σ^* hyperon resonances, Phys. Rev. C **92**, 025205 (2015); **95**, 049903(E) (2017).
[19] J. A. Oller and U. G. Meissner, Chiral dynamics in the presence of bound states: Kaon nucleon interactions revisited, Phys. Lett. B **500**, 263 (2001).
[20] D. Jido, J. A. Oller, E. Oset, A. Ramos, and U.-G. Meißner, Chiral dynamics of the two $\Lambda(1405)$ states, Nucl. Phys. **A725**, 181 (2003).
[21] J. Bulava *et al.* (Baryon Scattering (BaSc) Collaboration), Two-pole nature of the $\Lambda(1405)$ resonance from lattice QCD, Phys. Rev. Lett. **132**, 051901 (2024).
[22] F.-K. Guo, P.-N. Shen, and H.-C. Chiang, Dynamically generated 1^+ heavy mesons, Phys. Lett. B **647**, 133 (2007).
[23] A. Denig, F.-K. Guo, C. Hanhart, and A. V. Nefediev, Direct X(3872) production in e^+e^- collisions, Phys. Lett. B **736**, 221 (2014).
[24] V. Baru, X.-K. Dong, M.-L. Du, A. Filin, F.-K. Guo, C. Hanhart, A. Nefediev, J. Nieves, and Q. Wang, Effective range expansion for narrow near-threshold resonances, Phys. Lett. B **833**, 137290 (2022).
[25] R. Aaij *et al.* (LHCb Collaboration), Study of the lineshape of the $\chi_{c1}(3872)$ state, Phys. Rev. D **102**, 092005 (2020).
[26] M. Nauenberg and A. Pais, Woolly cusps, Phys. Rev. **126**, 360 (1962).
[27] E. Braaten and M. Lu, Line shapes of the $X(3872)$, Phys. Rev. D **76**, 094028 (2007).

[28] J. Nieves and M. P. Valderrama, The heavy quark spin symmetry partners of the $X(3872)$, Phys. Rev. D **86**, 056004 (2012).

[29] F.-K. Guo, C. Hidalgo-Duque, J. Nieves, and M. P. Valderrama, Consequences of heavy quark symmetries for hadronic molecules, Phys. Rev. D **88**, 054007 (2013).

[30] V. Baru, E. Epelbaum, A. A. Filin, C. Hanhart, U.-G. Meißner, and A. V. Nefediev, Heavy-quark spin symmetry partners of the $X(3872)$ revisited, Phys. Lett. B **763**, 20 (2016).

[31] P.-P. Shi, V. Baru, F.-K. Guo, C. Hanhart, and A. Nefediev, Production of the $X(4014)$ as the spin-2 partner of $X(3872)$ in e^+e^- collisions, Chin. Phys. Lett. **41**, 031301 (2024).

[32] M. Ablikim *et al.* (BESIII Collaboration), Future physics programme of BESIII, Chin. Phys. C **44**, 040001 (2020).

[33] M. Achasov *et al.*, STCF conceptual design report (Volume 1): Physics & detector, Front. Phys. **19**, 14701 (2024).